



Structural and Optical Properties of Nanocrystalline Tin Sulfide Thin Films Deposited By Thermal Evaporation

KEYWORDS

Thin films, vapor deposition, atomic force microscopy, X-ray diffraction, optical properties.

A. Salem

Physics Department, Faculty of Science, SouthValleyUniversity, Qena, Egypt

A. S. Salwa

Physics Department, Faculty of Science, KingKhalidUniversity, Abha, SaudiaArabiaKingdom.

S. N. Alamri

Department of Physics, Faculty of Education, TaibahUniversity, SaudiaArabiaKingdom.

ABSTRACT

Thermal evaporation technique was used to fabricate the nanocrystalline tin sulfide (SnS) thin films of thicknesses 200 nm and 377 nm on good quality glass substrate. The various physical properties of deposited thin films were investigated using X-ray diffraction (XRD), Atomic force microscopy (AFM), and ultraviolet-visible-near infrared spectroscopy at room temperature. X-ray diffraction analysis confirmed the orthorhombic phase of SnS films and the calculated lattice parameters were calculated. The grain size, dislocation density and micro strain were calculated using X-ray data. The result from AFM analysis show that the surface of films was compact, dense and smooth. The optical band gap and types of transitions involved in the absorption process was investigated. For allowed direct and indirect transition the band gap values varied in the range from 1.96 - 1.72 eV and 1.58 - 0.92 eV, respectively. The deduced values of the band gap suggest that the deposited thin films can be used in the fabrication of solar cell devices.

1. Introduction

The search for thin film materials for solar energy conversion and other related applications has been of great interest in recent past. Many efforts have been made towards using metal chalcogenides as this class of materials which shows somewhat superior performance when compared to others.

Among the important binary semiconductors of IV-VI group, the chalcogenides formed with Sn, especially Tin Sulfide compounds (SnS) have attracted considerable attention because of their physical properties, which are suitable for optoelectronic devices. SnS has particularly generated interest because of its nontoxic nature and absorption tunable band gap in the visible range. SnS thin films was prepared by various methods such as plasma enhanced chemical vapor deposition (PECVD), vacuum evaporation, chemical bath deposition, electrodeposition, and spray pyrolysis [1-11] with the purpose of manufacturing thin films suitable for using as a solar absorber in photovoltaic applications.

Due to the increasing interest of SnS, the current investigation attempts to find out ways of growing good quality SnS thin films with better properties for photovoltaic and solar cell applications using thermal evaporation under vacuum and controlled deposition conditions with attention given to its structural and optical properties.

In this work, the physical properties of the SnS thin films deposited by thermal evaporation have been investigated.

2. Experimental procedures

The compound prepared as a block compound by using Bridgman-Stockbarger method. In this method, the ampoule charged with required amount of pure Tin (Aldrich Mark 99.999%) and pure sulfur (Aldrich Mark 99.999%) according to the atomic weight of compound. After the compound SnS prepared as polycrystalline compound, thermally evaporated to have a thin film samples. Thin films of SnS were deposited by thermal evaporation using

molybdenum boat on glass substrates at room temperature with thickness 200 nm and 377 nm. The thicknesses of the films were measured with a Dektak 150 surface profiler. Structural properties of tin sulfide films were studied by X-ray diffraction (XRD) using a diffractometer Shimadzu 6000 (XRD-6000) with a CuK α line ($\lambda = 1.5405 \text{ \AA}$) with 2θ ranging from 5° to 90° . The X-ray tube voltage and current were 40 kV and 30 mA, respectively. The speed of the detector was 1° per min.

The surface morphology of the deposited films was examined using atomic force microscopy (AFM, Veeco CP-II) in non-contact mode with Si tips at a scan rate of 1 Hz (AFM image for 377 nm thin film). The transmittance, $T(\lambda)$, and reflectance, $R(\lambda)$ spectra of the deposited films were measured at a normal and 5° incident angle, respectively. These measurements were acquired in air at room temperature using a computer-aided double beam spectrophotometer (Shimadzu 3150 UV-VIS-NIR). The absorption coefficient (α) was calculated from $T(\lambda)$ and $R(\lambda)$ measurements and from its dependence on the photon energy ($h\nu$), The optical band gap E_g was obtained.

3. Results and discussion

3.1. Morphology and Structural analysis.

Fig.1 shows the recorded XRD pattern of the deposited SnS thin film prepared on glass substrate at room temperature. All reflections can be indexed to pure orthorhombic SnS phase as compared with the JCDPS 83-1758 with no impurities peaks such as elemental tin, sulfur and other tin sulfide phases, indicating the formation of single phase SnS. The 2θ peaks observed at 31.4° , 39.0° , 42.96° , 51.36° , and 54.62° exhibit the formation of the orthorhombic phase of SnS which correspond to the (111), (131), (002), (151), and (042) planes of reflections. The strongest peak for the grown films in Fig.1 occurred at $2\theta = 31.4^\circ$ with $d = 2.851 \text{ \AA}$ which corresponds to (111). The different peaks in the diffractogram were indexed and the corresponding values of inter-planar spacing 'd' were calculated and

compared with the standard values [12] JCPDS Diffraction DataCard No. 89-0253.]. The inter-planar distances as were indicated in the XRD result were found to be 2.69 Å, 4.178 Å, 2.553 Å, and 2.627 Å. The presence of the large number of peaks indicates that the film is polycrystalline in nature and good crystalline structure because of sharp structural peaks. From X-ray diffraction data, the crystallite size of the deposited film was calculated using Debye-Scherrer formula [12].

The Miller indices (hkl) relate the interplanar distance d_{hkl} or d-spacing to the lattice parameters by an equation specific to the crystal system. For example, in a structure with an orthorhombic unit cell the relationship is given by [13]:

$$\frac{1}{d_{hkl}^2} = \frac{h^2}{a^2} + \frac{k^2}{b^2} + \frac{l^2}{c^2}$$

(1)

According to the data of the XRD peaks, we calculated the lattice parameters (a, b and c) of the SnS film. The evaluated lattice parameters of the SnS film are a = 4.148 Å, b = 11.48 Å, and c = 4.177 Å [14], the broadening of peaks of XRD pattern are inversely proportional to the average crystallite size (D):

$$D = \frac{K\lambda}{\beta \cos \theta}$$

(2)

where D is the grain size, λ is the wavelength of the CuK radiation used ($\lambda = 1.5405 \text{ \AA}$), K is a constant generally taken to have the value 0.9 [15], β is the full width at half maximum FWHM of the reflection peak that has the same maximum intensity in the diffraction pattern, and θ is the diffraction angle of x-rays.

For the fabrication of good quality thin film to use in optical devices, it is necessary to reduce the surface roughness and dislocation density of the SnS film. So the value of the dislocation density (δ), which gives the number of defects in the film was calculated from the average values of the crystallite size D by the Williamson and Smallman's formula [16]:

$$\delta = \frac{1}{D^2} \quad \text{lines/m}^2$$

(3)

The micro strain (ϵ) is obtained using the relation

$$\epsilon = \frac{1}{D^2} \quad \text{lines/m}^2$$

(4)

All these parameters, the (hkl) plane, FWHM value, grain size (D), dislocation density (δ), and the micro strain (ϵ) values of SnS thin film are calculated and presented in Table 1.

Fig.2 depicts the AFM image of the SnS thin film (AFM image for 377 nm thin film), the mean roughness of SnS surfaces was approximately 10.8 nm. The value of the rough-

ness was calculated by the program of the instrument.

3.2. Optical Properties.

Optical properties are very important for solar cell materials. Fig.3 shows the optical transmission spectra $T(\lambda)$ for SnS thin films of thickness 200 nm and 377 nm in the wavelength range from 400-1200 nm.

Fig.4 illustrates the optical reflection $R(\lambda)$ spectra for SnS thin films of thickness 200nm and 377 nm in the wavelength range from 400- 1200 nm. The transmission $T(\lambda)$ through an absorbing slab is related to its reflectivity $R(\lambda)$, thickness d and the absorption coefficient α by

$$T = (1 - R) \exp -\alpha d$$

(5)

In order to estimate the optical band gap, the following equation can be used:

$$(\alpha h\nu) = A(h\nu - E_g)^n$$

(6)

where E_g is the energy band, α is the absorption coefficient, A is a constant and n characterizes the transition process which has a values n = 1/2 and 3/2 for direct allowed and forbidden transitions, respectively. n = 2 and 3 for indirect allowed and forbidden transitions, respectively.

Fig.5 shows the plot of $(\alpha h\nu)^2$ vs. photon energy for SnS thin films of thickness 200 nm and 377 nm respectively. It is clear from this figure that each curve tends to a straight line in the high photon energy region. By extrapolating the straight line from this linear region, E_g was estimated by the intercept with the energy axis. The values of the direct allowed transition for both thickness 200 nm, 377 nm is 1.96 eV and 1.58 eV, respectively. Also, it is clear from this figure that the thinner (200 nm) has a large direct band gap of 1.96 eV. Because too thin films result in larger transmission in the shorter wavelength, this agrees with reference [17]. To calculate the wavelength corresponding to direct band gap using the eq. $E = h\nu$ where h Planck constant and ν frequency $E = hc/e\lambda$ e electron charge, c speed of light and λ wavelength, E energy

$$\text{So } \lambda = \frac{hc}{eE} = \frac{6.6 \times 10^{-34} \times 3 \times 10^8}{1.6 \times 10^{-19} \times 1.96}$$

$$\lambda = 6.313 \times 10^{-7} \text{ m}$$

$$\lambda = 6.313 \times 10^{-7} \times 10^{10} = 6313 \text{ \AA}$$

So this value is in visible light spectrum range

And for $E_g = 1.58 \text{ eV}$

$$\lambda = \frac{7.832 \times 10^{-7} \times 10^{10}}{1} = 7832 \text{ \AA}$$

Fig.6 shows the plot of $(\alpha h\nu)^{1/2}$ vs. photon energy for SnS thin films of thickness 200 nm and 377 nm, respectively. The indirect band gap E_{ind} is often estimated by the intercept of the energy axis at $(\alpha h\nu)^{1/2} = 0$, it has the values of 1.72 eV and 0.92 eV for samples of thickness 200 nm and 377 nm, respectively. Table (2) shows the total values of direct and indirect energy gaps of the present work these

values agree well with other published results reported by E. Guneri et al [18] in which band gap values varied in the range 1.3 - 1.97 eV for allowed direct transition and from 0.83 - 1.36 eV for allowed indirect transition. The deduced values of the band gap in the present work are optimized values for the solar absorber in solar cell devices.

This paper interest to the effect of different thickness in structure and optical properties of SnS. These thicknesses have not studied before. The reported direct and indirect optical band gap energies for SnS thinfilms varied in the range of 1.2 - 2 eV and 0.8 - 1.2 eV, respectively [19, 20]. Albers et al [21] reported indirect band gap of SnS single crystal is 1.07 eV, whereas it is 1.1 eV as reported by Nasary [22].

4. Conclusion

In this manuscript, Nanocrystalline tin sulfide thin films with thicknesses 200 nm and 377 nm have been deposited on glass substrates at room temperature by thermal evaporation. Morphology and structure characterization of films were investigated using AFM and XRD. The films exhibit SnS phase in a crystalline in nature. The optical properties of SnS thin films of thickness 200 nm and 377 nm were investigated. The films have two transition band gap direct and indirect band gap. These polycrystalline, single-phase and highly absorbing SnS thin films are suitable for the solar absorber in solar cell devices.

Fig. 1. The XRD pattern of the SnS films.

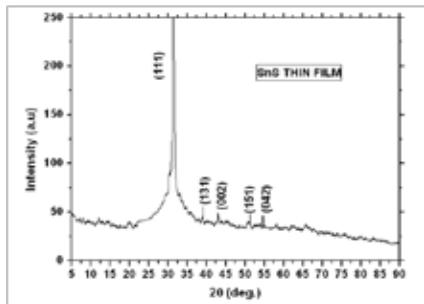


Fig. 2. AFM image for 377 nm thin film.

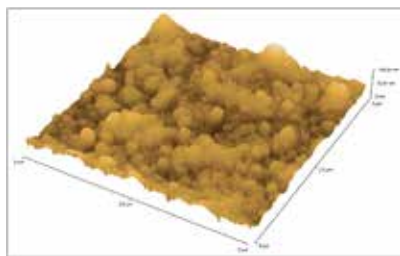


Fig. 3. Transmission spectra (T) of SnS thin films.

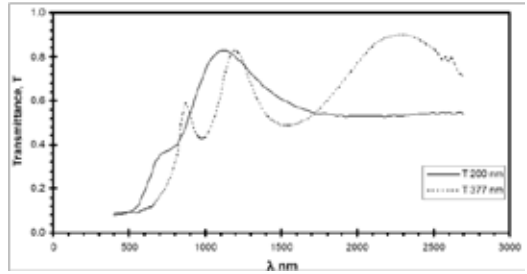


Fig. 4. Reflection spectra (T) of SnS thin films.

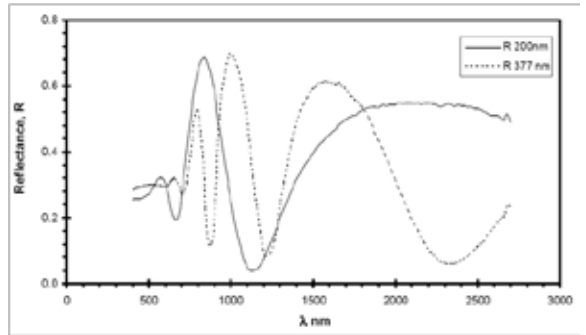


Fig. 5. (ahv)² vs. hv of SnS thin films.

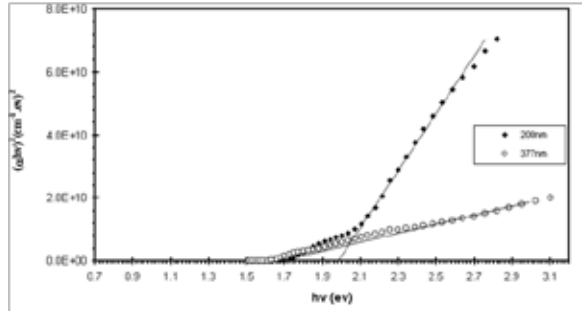
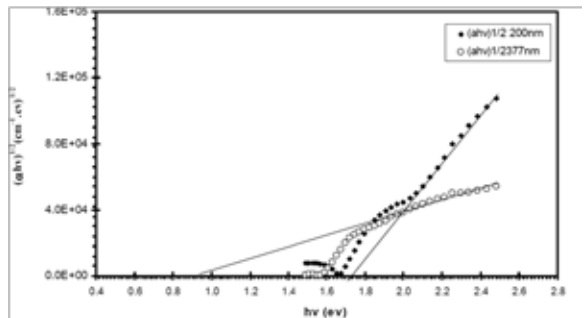


Fig. 6. (ahv)^{1/2} vs. hv of SnS thin films.



2θ (degree)	d Å (spacing)	β (FWHM)	hkl	Grain Size (D) nm	Density (δ) x 10 ³ Lines/m ²	Micro strain (ε) x 10 ⁻³
31.4	2.851	0.5	111	16.6	360	210
39.0	2.332	0.11	131	84	14	45
42.96	2.089	0.12	002	214	2.18	49
51.36	1.346	0.114	151	71.4	19.6	37
54.6	1.689	0.123	042	71.8	19.4	8

Table 1: The (hkl) plane, FWHM value, grain size (D), dislocation density (δ), and the

micro strain (ε) values of SnS thin film.

REFERENCE

- [1] B. Thangaraju, P. Kaliannam, J. Phys.D: Appl. Phys. 33 (2000) 1054. | [2] N. Koteswara Reddy, K. T. Ramakrishna Reddy, Thin Solid Films 325 | (1998) 4.. | [3] P. Pramanik, P. K. Basu, S. Biswas Thin Solid Films 150 (1987) 269. | [4] Z. Zainal, M. Z. Hussein, A. Ghazali, Solar Energy Matter. Solar Cells | 40 (1996) 347. | [5] A. Ghazali, Z.Zainal, M. Z. Hussein, A. Kasseim, Solar Energy Matter. | Solar Cells 55(1998) 237. | [6] K. Deraman, S. Sakrani, B. B. Ismail, Y. Wahab, R. D. Gould, Int. J. | Electron. 76 (5)(1994) 917. | [7] A. Ortiz, J. C. Alonso, M. Garcia, J. Toriz, Semicond. Sci. Technol. 11 | (1996) 243. | [8] B. Ghosh, M. Das, P. Banerjee, S. Das, Sol. Energy Matter. Sol. Cells | 92 (2008) 1099. | [9] D. Avellaneda, M. T. S. Nair, P. K. Nair, J. Electrochem. Soc. 155 (2008) | D 525. | [10] N. Sato, M. Ichimura, E. Arai, Y. Yamazaki, Sol. Energy Matter. Sol. | Cells 85 (2005) 153. | [11] K. T. R. Reddy, N. K. Reddy, R. W. Miles, Sol. Energy Matter. Sol. | Cells 90 (2006) 3041. | [12] B. D. Cullity, in Elements of X-ray diffraction 2nd Edition, Addison | Wesley, [1978] | [13] B. Cullity, Elements of X-ray diffraction, Addison-Wesley Publishing | Company Inc., USA, 1967, pp. 501. | [14] G. Willeke, R. Dasbach, B. Sailer, E. Bucher, Thin Solid Films 213, 271 | (1992). | [15] H. Jensen, J. H. Pedersen, J. E. Jorgensen, J. Skov Pedersen, K.D | Joensen, S.B. Iversen, E.G. Sogaard, J. of Experimental Nanoscience, | 1 (2006) 355]. | [16] G. B. Williamson, R. C. Smallman, Philos. Mag. 1, 34 (1956) -46. | [17] M.Devika, N. Koteeswara Reddy, K. Ramesh, R.Ganesan, K. R. Gu- | nasekhar, E. S. R. Gopal, K. T. Ramakrishna Reddy J.Electrochem. | Soc.154 (2007) H67. | [18] E. Guneri, C. Ulutas, F. Kirmizigul, G. Altindemir, F.Gode, C.Gumus, | Applied Surface Science 257 (2010) 1189-1195. | [19] S. Lopez, A. Ortiz, Semicond. Sci. Technol. 9 (1994) 2130. | [20] M. Devika, N. Koteeswara Reddy, D. Sreekantha Reddy, Q. Ahsanul- | haq, K. Ramesh, E. S. R. Gopal, K. R. Gunasekhar, Y.B. Hahn, J. | Electrochem. Soc. 155 (2008) H130. | [21] W. Albers, C. Haas, H. ober, G.R. Schodder, J. D. Wasscher, J.Phys. | Chem. Solids 23 (1962) 215. | [22] M. M. Nassary, J. Alloys compd. 398 (2005) 21. |